

## Article

# A Numerical Study on the Electrochemical Treatment of Chloride-Contaminated Reinforced Concrete

Yanan Xi <sup>1</sup>, Yun Gao <sup>2,\*</sup>, Wenwei Li <sup>3</sup> and Dong Lei <sup>1</sup><sup>1</sup> College of Mechanics and Materials, Hohai University, Nanjing 211100, China<sup>2</sup> School of Human Settlements and Civil Engineering, Xi'an Jiaotong University, Xi'an 710049, China<sup>3</sup> Division of Science and Technology Management, China Three Gorges Corporation, Beijing 110108, China

\* Correspondence: yun.gao@xjtu.edu.cn

**Abstract:** Electrochemical treatment, specified as electrochemical chloride extraction (ECE), is one of the common techniques developed for the rehabilitation of chloride-contaminated reinforced concrete. In practice, ECE is time-consuming; for instance, the treatment duration could last several weeks or even longer. In order to reduce the laboratory work, this paper presents some results about a numerical study of the ECE. It is to solve a series of physical equations governing multiple ionic transport making use of a finite difference method. The effects of some critical factors are discussed in detail, such as the treatment duration, the current density and the cover thickness. In addition, for the sake of validation, the numerical results are also compared with those obtained from an experimental test.

**Keywords:** electrochemical chloride extraction; finite difference method; treatment duration; current density; cover thickness



**Citation:** Xi, Y.; Gao, Y.; Li, W.; Lei, D. A Numerical Study on the Electrochemical Treatment of Chloride-Contaminated Reinforced Concrete. *Modelling* **2022**, *3*, 374–384. <https://doi.org/10.3390/modelling3030024>

Academic Editor: Filippo Ubertini

Received: 31 May 2022

Accepted: 16 August 2022

Published: 22 August 2022

**Publisher's Note:** MDPI stays neutral with regard to jurisdictional claims in published maps and institutional affiliations.



**Copyright:** © 2022 by the authors. Licensee MDPI, Basel, Switzerland. This article is an open access article distributed under the terms and conditions of the Creative Commons Attribution (CC BY) license (<https://creativecommons.org/licenses/by/4.0/>).

## 1. Introduction

The chloride-induced corrosion of steel in reinforced concrete is a worldwide engineering problem, since it brings a severe threat to the service life of infrastructure. Generally, steel in concrete is protected by a passive film. However, the presence of some kinds of aggressive species, for instance, the chloride ions, could accelerate the breakdown of the passive film. As a result, the ingress of moisture and oxygen would initiate the corrosion process. In fact, much evidence suggests that the concentration of the chloride ion at the steel surface has to reach a certain level, i.e., the chloride threshold level, for the corrosion to take place [1–4]. This means that the control of the chloride content below the threshold level might be an efficient approach for prohibiting the corrosion of the reinforcing steel.

Electrochemical treatment, specified as electrochemical chloride extraction (ECE), is one of the common techniques developed for the rehabilitation of chloride-contaminated reinforced concrete. In principle, when subjected to an externally applied electric field, the negatively charged chloride ions are transferred in the direct current away from the steel bar toward the positively charged anode. That is, the reinforcing steel acts as the cathode, while an external anode is placed in a suitable electrolyte at the surface of the concrete cover. The purpose is to control the chloride content within the reinforced concrete until below the chloride threshold level, and therefore the corrosion of the reinforcing steel can be prohibited [5–7].

Over the last three decades, a number of experimental tests have been performed about the ECE [8–12]. Results indicate that if applied in an appropriate way, the electrochemical treatment can lead to a substantial reduction in the chloride profile of the cover zone as well as the corrosion rate of steel in the short term. Nevertheless, if it was applied too late, the electrochemical treatment cannot assure the re-passivation of the corroded steel. In addition, significant alterations might be encountered after the electrochemical treatment about the microstructure of the cementitious matrix as well as the chemical composition of the pore

solution [13,14]. For experimental tests, some critical parameters such as the treatment duration, the current density and the cover thickness are of paramount importance to the final effect of the ECE [15–18].

Along with laboratory and field tests, considerable efforts have also been spent on the numerical modelling of the ECE. The former could last several weeks or even longer, while the latter needs much less work. For instance, Andrade et al. proposed the basic equations and solved them for the cases of chloride concentration being constant or following the error function trend [19]. Based on that, Castellote et al. studied the effects of testing conditions and treatment duration [20,21]. Buenfeld et al. discussed the general experimental situations of chloride transport in concrete subjected to an electric field that may be applicable to the ECE, the cathodic protection and the rapid chloride diffusion test [22]. Li and Page developed a unified transport model for multiple ionic species, which was then solved by means of a finite element method [23,24]. Liu et al. employed the transport model for multiple ionic species and took more factors into account, such as the aggregate content, shape and gradation, the coupled environmental actions, and so on [25–27].

In order to reduce the laboratory work, a numerical study of the ECE is performed in this work, which relies on the governing equations of the multiple ionic transport as introduced by Li and Page [23,24]. Different from Li and Page [23,24] and Liu et al. [25–27], a finite difference method is adopted and implemented. The effects of some critical factors are discussed in detail, such as the treatment duration, the current density and the cover thickness. The main contents are organized as follows. Section 2 describes the modeling framework of the ECE including the governing equations as well as the finite difference algorithm. Section 3 presents the numerical results. Section 4 compares the numerical results with those obtained from an experimental test. It should be pointed out that the current paper does not aim to demonstrate the advantages or disadvantages of the finite difference scheme, but shows another kind of option other than the existing finite element scheme when the numerical modeling of the ECE is performed.

## 2. Modeling Framework of the ECE

### 2.1. The Governing Equations

As shown in Figure 1, the ECE can be implemented on a cylindrical specimen where the reinforcing steel rod is centrally embedded within the concrete cover. The negative terminal is connected to the steel, and the positive terminal is connected to the titanium mesh. Upon the current circuit, the steel achieves negative polarity that repulses anions and attracts cations.

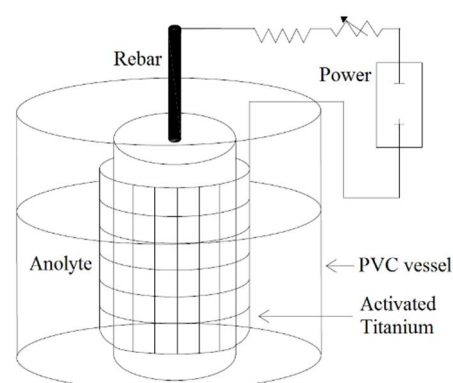


**Figure 1.** Schematic illustration of the ECE.

In the present model, five major ionic species are taken into account, i.e.,  $\text{Cl}^-$ ,  $\text{Na}^+$ ,  $\text{K}^+$ ,  $\text{Ca}^{2+}$ , and  $\text{OH}^-$ . The concrete cover is considered as a homogeneous medium, and the

transport of ionic species can then be described by a series of physical laws in terms of the equations of continuity, flow, current and electroneutrality as follows [24]:

$$\frac{\partial C_i}{\partial t} + \frac{\partial S_i}{\partial t} = -\nabla J_i \quad (1)$$

$$J_i = -D_i \nabla C_i - z_i D_i \left( \frac{F}{RT} \nabla U \right) C_i \quad (2)$$

$$I = F \sum_i z_i J_i \quad (3)$$

$$\sum_i z_i C_i = 0 \quad (4)$$

where  $C_i$  is the concentration of free ions,  $S_i$  is the concentration of bound ions,  $t$  is the treatment duration,  $J_i$  is the flux,  $D_i$  is the apparent diffusion coefficient in concrete,  $z_i$  is the charge number,  $F = 96,500$  C/mol is the Faraday constant,  $R$  is the gas constant,  $T$  is the temperature,  $U$  is the potential,  $I$  is the current density,  $i$  is the index of ionic species. Note that the equation of flow takes the terms of diffusion and migration into account, while the term of convection is neglected. Substituting Equation (2) into Equations (1) and (3) yields that

$$\frac{\partial C_i}{\partial t} + \frac{\partial S_i}{\partial t} = \nabla \left[ D_i \nabla C_i + z_i D_i \left( \frac{F}{RT} \nabla U \right) C_i \right] \quad (5)$$

$$\left( \frac{F}{RT} \nabla U \right) = - \frac{I/F + \sum_i (z_i D_i \nabla C_i)}{\sum_i (z_i^2 D_i C_i)} \quad (6)$$

The concentrations of bound ions are set to zero except that of the chloride ion. Herein, the chloride binding with solid cementitious phase is accounted for by means of the classic Langmuir isotherm as follows [28]:

$$S_{Cl} = \frac{\alpha C_{Cl}}{w(1 + \beta C_{Cl})} \quad (7)$$

where  $w$  is the content of the water expressed per unit weight of cement;  $\alpha = 0.42$  and  $\beta = 0.8$  L/mol are constants [28].

For the completion of the numerical model, the boundary conditions might be written as follows:

$$\text{Cathode : } J_{OH} = \frac{I_0}{z_{OH} F}; \quad J_i = 0, \quad i \neq OH \quad (8)$$

$$\text{Anode : } J_{Cl} = \frac{I_1}{z_{Cl} F}; \quad J_i = 0, \quad i \neq Cl \quad (9)$$

where  $I_0$  and  $I_1$  is the current density at the external surface of the steel rod and the concrete cover, respectively.

## 2.2. Finite Difference Algorithm

Different from previous authors, a finite difference method is implemented to provide the numerical solution of the ECE. The governing equations, i.e., Equations (5) and (6) are rewritten as follows:

$$\frac{\partial C_i}{\partial t} = -\xi_i \nabla J_i \quad (10)$$

$$J_i = -D_i \nabla C_i + z_i D_i \left[ \frac{I/F + \sum_i (z_i D_i \nabla C_i)}{\sum_i (z_i^2 D_i C_i)} \right] C_i \quad (11)$$

where  $\zeta_i$  is the coefficient related to free and bound ions. It holds that

$$\begin{cases} \zeta_{Cl} = \frac{(1+\beta C_{Cl})^2}{(1+\beta C_{Cl})^2 + \alpha/w}; & i = Cl \\ \zeta_i = 1; & i \neq Cl \end{cases} \quad (12)$$

For the cylindrical shape of the reinforced concrete specimen, the current field within the concrete cover is assumed to be radial, and thus the local current density can be obtained from

$$I = I_0 \frac{r_0}{r_0 + r} \quad (13)$$

where  $r_0$  is the radius of the steel rod and  $r$  is the distance from the steel surface.

Out of the convenience, a polar coordinate system is established that originates from the centre of the steel rod. Then, the discretization is performed at both the spatial and time domains. Let  $\delta r$  and  $\delta t$  be the spatial and time increments, respectively. The concentration is defined at each element, while the flux is defined at each interface between neighbouring elements, as indicated in Figure 2. The concentration and flux are written as  $C_i^k(j) = C_i(j \cdot \delta r, k \cdot \delta t)$  and  $J_i^k(j) = J_i(j \cdot \delta r, k \cdot \delta t)$ , where the positive integers  $j$  and  $k$  are the indices denoting the discretization at the spatial and time domains. For the polar coordinate system, the partial derivatives of concentration and flux are expressed as follows:

$$\frac{\partial C_i^k}{\partial t} = \frac{C_i^{k+1}(j) - C_i^k(j)}{\delta t} \quad (14)$$

$$\nabla C_i^k = \frac{C_i^k(j) - C_i^k(j-1)}{\delta r} + \frac{C_i^k(j) + C_i^k(j-1)}{2(r_0 + j \cdot \delta r)} \quad (15)$$

$$\nabla J_i^k = \frac{J_i^k(j+1) - J_i^k(j)}{\delta r} + \frac{J_i^k(j+1) + J_i^k(j)}{2(r_0 + j \cdot \delta r)} \quad (16)$$

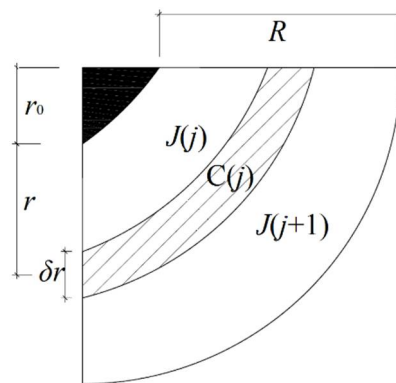


Figure 2. Schematic illustration of the finite difference method.

Substitute Equations (14)–(16) into the governing equations, and then the concentrations and fluxes of ionic species can be explicitly solved by means of the successive iterations. Note that in order to satisfy the electroneutrality condition, the concentration of the hydroxyl ion shall be adjusted after each loop.

### 3. Numerical Results

#### 3.1. Model Parameters

The finite difference algorithm might be implemented with  $\delta r = 0.1$  mm and  $\delta t = 60$  s. Other parameters are listed in Table 1 which are necessary for the implementation of the numerical model, including initial concentrations, diffusion coefficients, charge numbers and molar masses of free ions. Among them, the initial ionic concentrations were adopted

from [29]. The diffusion coefficients were taken from [30,31]. It can be noted that the cations ( $\text{Na}^+$ ,  $\text{K}^+$ ,  $\text{Ca}^{2+}$ ) are much less mobile than the anions ( $\text{Cl}^-$ ,  $\text{OH}^-$ ).

**Table 1.** Parameters for the multiple ionic transport model.

Ions	$\text{Cl}^-$	$\text{Na}^+$	$\text{K}^+$	$\text{Ca}^{2+}$	$\text{OH}^-$
Initial concentration (mmol/L)	265.0	507.5	33.1	562.5	1400.6
Diffusion coefficient ( $10^{-12} \text{ m}^2/\text{s}$ )	25	0.3	1	0.15	40
Charge number	-1	1	1	2	-1
Molar mass (g/mol)	35.5	23	39	40	17

### 3.2. Effect of the Treatment Duration

Figure 3 shows the concentration profiles of cations ( $\text{Cl}^-$ ) and anions ( $\text{Na}^+$ ) within the concrete cover after 4, 8, and 12 weeks of the electrochemical treatment. For that, the current density  $I_0$  is  $1.0 \text{ A/m}^2$  and the cover thickness  $R$  is 50 mm.

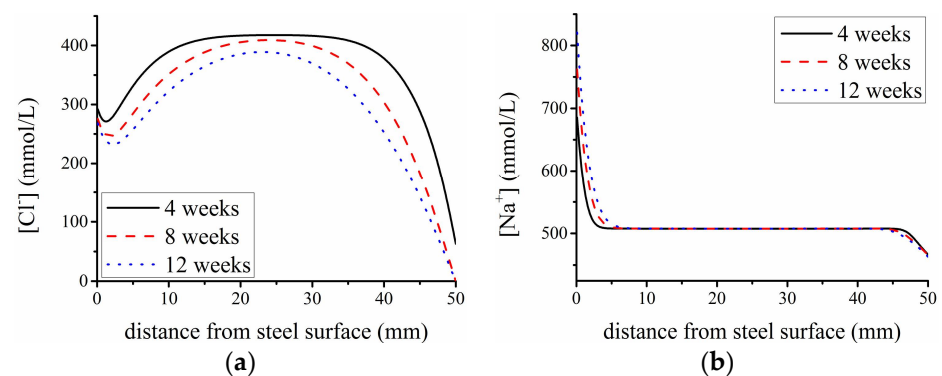


**Figure 3.** The concentration profiles of cations and anions within the concrete cover after 4, 8, and 12 weeks of the electrochemical treatment (a)  $\text{Cl}^-$ ; (b)  $\text{Na}^+$ .

A remarkable reduction is detected for the chloride content after the electrochemical treatment. Moreover, the chloride content is much lower in the close vicinity of cathode (i.e.,  $r \rightarrow 0 \text{ mm}$ ) or anode (i.e.,  $r \rightarrow 50 \text{ mm}$ ) than that at the central area of the concrete cover (i.e.,  $r \rightarrow 25 \text{ mm}$ ). Anions such as  $\text{Na}^+$  tend to be accumulated at the cathode and depleted at the anode as the treatment duration is increased. Table 2 lists the mean concentrations of cations ( $\text{Cl}^-$ ) and anions ( $\text{Na}^+$ ,  $\text{K}^+$ ,  $\text{Ca}^{2+}$ ) in the vicinity of the steel surface (i.e.,  $r < 5 \text{ mm}$ ). It is found that as the treatment duration is increased from 4 to 8 to 12 weeks, the chloride content is reduced from 29% to 37% to 42%. In other words, compared to the first 4 weeks, the later 8 weeks demonstrates a much lower efficiency in the chloride extraction. Since the concentrations of  $\text{Na}^+$  and  $\text{K}^+$  are increased rapidly with the treatment duration, it can result in the risk of the alkali aggregate reaction (AAR). In this regard, it is suggested that the treatment duration should not last more than 8 weeks for experimental tests. This agrees with the previous reports that after 6–10 weeks of application, ECE can remove 30–80% chloride content in concrete [14].

**Table 2.** Mean ionic concentrations in the vicinity of steel after the electrochemical treatment of different treatment durations.

Treatment Duration (Weeks)	$\text{Cl}^-$ (mmol/L)	$\text{Na}^+$ (mmol/L)	$\text{K}^+$ (mmol/L)	$\text{Ca}^{2+}$ (mmol/L)
4	296.4	534.4	38.9	587.0
8	260.9	560.8	44.4	611.0
12	242.8	586.2	49.3	634.3

### 3.3. Effect of the Current Density

Figure 4 shows the concentration profiles of cations ( $\text{Cl}^-$ ) and anions ( $\text{Na}^+$ ) within the concrete cover for the current density  $I_0$  of 1, 3, and 5  $\text{A}/\text{m}^2$ . For that, the treatment duration  $t$  is 4 weeks and the concrete cover thickness  $R$  is 50 mm.

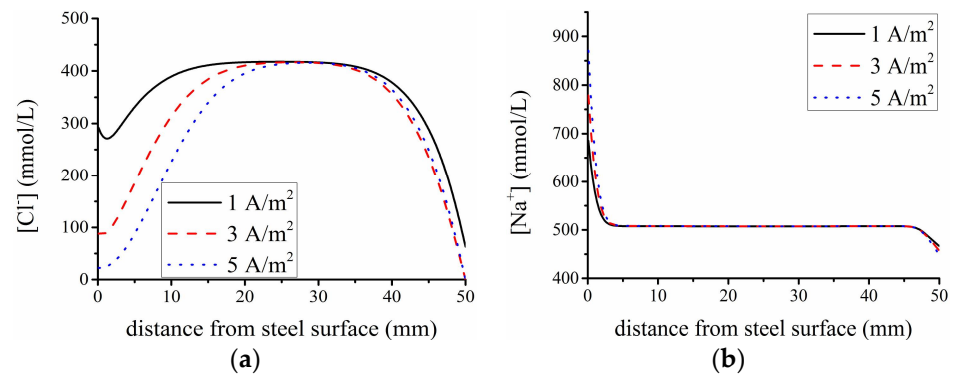


**Figure 4.** The concentration profiles of cations and anions within the concrete cover after 1, 3, and 5  $\text{A}/\text{m}^2$  of the electrochemical treatment (a)  $\text{Cl}^-$ ; (b)  $\text{Na}^+$ .

As the current density is increased from 1 to 3 to 5  $\text{A}/\text{m}^2$ , the chloride content sees a remarkable reduction in the close vicinity of cathode (i.e.,  $r \rightarrow 0$  mm) but is stable in the close vicinity of the anode (i.e.,  $r \rightarrow 50$  mm). Compared to the current density of 1  $\text{A}/\text{m}^2$ , the current density of 3 or 5  $\text{A}/\text{m}^2$  brings a rapid increase in the efficiency in the chloride extraction. Anions such as  $\text{Na}^+$  tend to be accumulated at the cathode and depleted at the anode as the current density is increased. Table 3 lists the mean concentrations of cations and anions in the vicinity of the steel surface (i.e.,  $r < 5$  mm). It is found that as the current density is increased from 1 to 3 to 5  $\text{A}/\text{m}^2$ , the chloride content is reduced from 29% to 69% to 88%. Nevertheless, this does not assure that a high current density can be applied without any restrictions, since it probably leads to the heat release as well as the hydrogen emission problem. Besides that, like the effect of the treatment duration, the concentrations of  $\text{Na}^+$  and  $\text{K}^+$  are increased rapidly with the current density, and special attention should be paid to the risk of the alkali aggregate reaction (AAR). In this regard, a current density  $1 < I_0 < 3 \text{ A}/\text{m}^2$  might be suggested for experimental tests.

**Table 3.** Mean ionic concentrations in the vicinity of steel after the electrochemical treatment of different current densities.

Current Density $I_0$ ( $\text{A}/\text{m}^2$ )	$\text{Cl}^-$ (mmol/L)	$\text{Na}^+$ (mmol/L)	$\text{K}^+$ (mmol/L)	$\text{Ca}^{2+}$ (mmol/L)
1	296.4	534.4	38.9	587.0
3	128.8	549.7	42.3	603.9
5	48.4	564.8	45.5	620.6

### 3.4. Effect of the Cover Thickness

Figure 5 shows the concentration profiles of cations ( $\text{Cl}^-$ ) and anions ( $\text{Na}^+$ ) within the concrete cover of 30 mm, 40 mm, and 50 mm in thickness. The treatment duration  $t$  is 4 weeks and the current density  $I_0$  is 1  $\text{A}/\text{m}^2$ . For the sake of comparison, the distance from the steel surface is normalized as  $r/R$ .

As the concrete cover thickness  $R$  is increased from 30 to 40 to 50 mm, the chloride content sees a gradual increase. That is, the efficiency for the chloride extraction from the reinforced concrete is decreased with the increase of the cover thickness. The reason can be attributed to the fact that for a smaller cover thickness, a shorter path results for the transport of chloride. Anions such as  $\text{Na}^+$  tend to be accumulated at the cathode and

depleted at the anode. Table 4 lists the mean concentrations of cations ( $\text{Cl}^-$ ) and anions ( $\text{Na}^+$ ,  $\text{K}^+$ ,  $\text{Ca}^{2+}$ ) in the vicinity of the steel surface (i.e.,  $r \rightarrow 3$  mm for  $R = 30$  mm,  $r \rightarrow 4$  mm for  $R = 40$  mm, and  $r \rightarrow 5$  mm for  $R = 50$  mm). It is found that unlike the treatment duration  $t$  or the current density  $I_0$ , the cover thickness  $R$  does not bring a detectable variation in the reduction of the chloride content in the vicinity of the steel surface. In this regard, if only the efficiency of the ECE is considered, there is no specific requirement about the cover thickness for experimental tests.

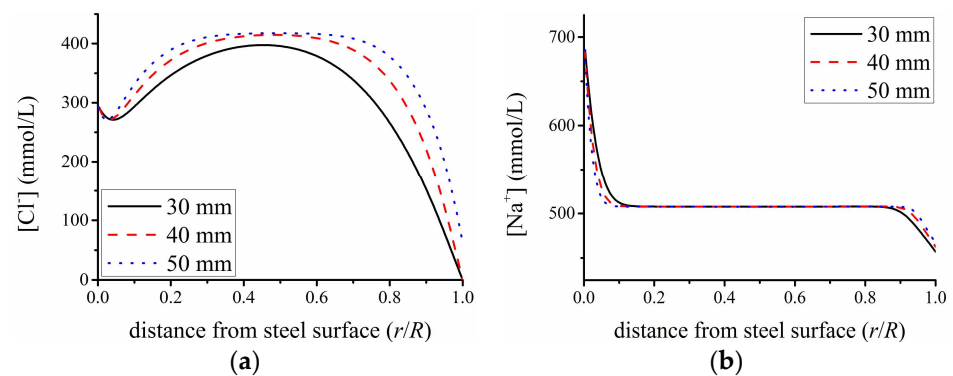


**Figure 5.** The concentration profiles of cations and anions within the concrete cover after  $1 \text{ A/m}^2$  and 4 weeks of the electrochemical treatment (a)  $\text{Cl}^-$ ; (b)  $\text{Na}^+$ .

**Table 4.** Mean ionic concentrations in the vicinity of steel after the electrochemical treatment of different cover thicknesses.

Cover Thickness (mm)	$\text{Cl}^-$ (mmol/L)	$\text{Na}^+$ (mmol/L)	$\text{K}^+$ (mmol/L)	$\text{Ca}^{2+}$ (mmol/L)
30	296.2	534.4	38.9	587.0
40	296.3	534.4	38.9	587.0
50	296.4	534.4	38.9	587.0

#### 4. Validation

The data collected from the experimental test performed by Fajardo et al. are chosen to validate the numerical modelling [29]. Besides the same specimen geometry shown in Figure 1 and the initial concentrations of free ions listed in Table 1, the height of the specimen was 110 mm and the cover thickness was  $R = 50$  mm. The current density was  $I_0 = 1 \text{ A/m}^2$ . The value of  $\rho$  and  $f$  was  $2.5 \text{ g/cm}^3$  and 12.9%, respectively.

As shown in Figures 6–8, the concentration profiles of the cation ( $\text{Cl}^-$ ) and the anion ( $\text{Na}^+$ ) within the concrete cover are compared between modelling and the experimental test at three specific stages, i.e., before the electrochemical treatment, after the electrochemical treatments of 21 days and 90 days.

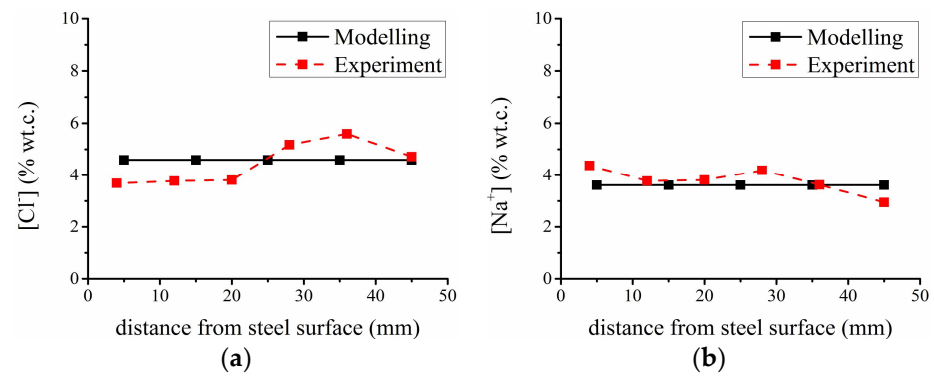


**Figure 6.** Comparison of the concentration profiles between modelling and the experimental test before the electrochemical treatment (a)  $Cl^-$ ; (b)  $Na^+$ .

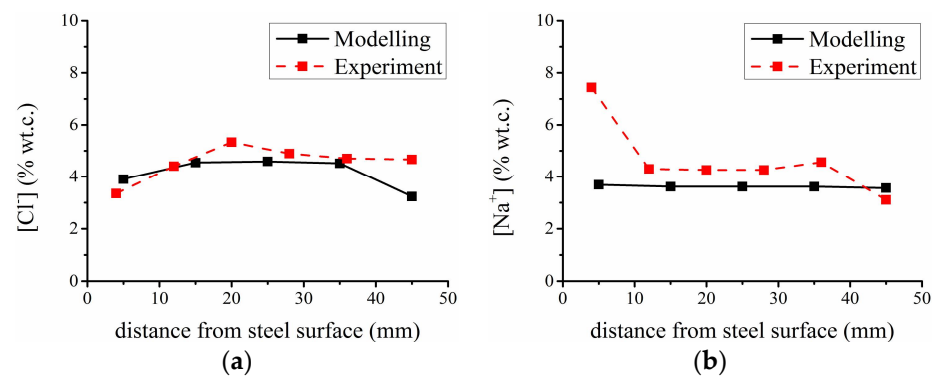


**Figure 7.** Comparison of the concentration profiles between modelling and the experimental test after the electrochemical treatment of 21 days (a)  $Cl^-$ ; (b)  $Na^+$ .

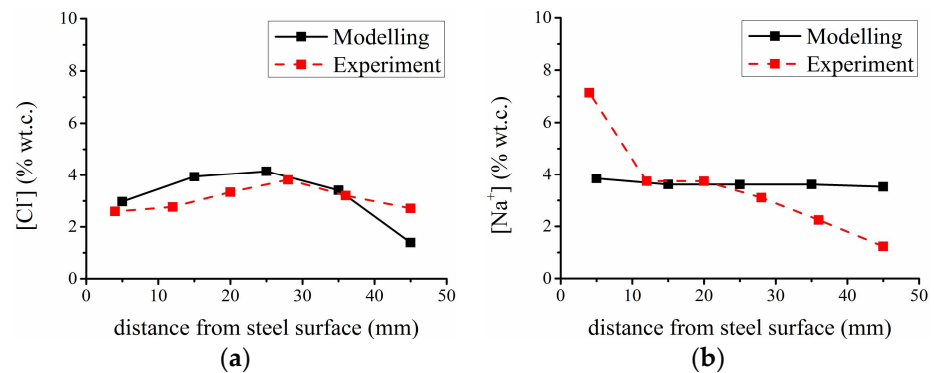


**Figure 8.** Comparison of the concentration profiles between modelling and the experimental test after the electrochemical treatment of 90 days (a)  $Cl^-$ ; (b)  $Na^+$ .

It can be noted that the overall trend of numerical modelling results agrees well with the experimental test, for instance, the concentration profiles of the cation ( $Cl^-$ ). Besides that, some discrepancies are also detected, particularly in the case of the concentration profiles of the anion ( $Na^+$ ). Herewith, two factors might be attributed to such a finding, i.e., the uncertainty of the ionic diffusion coefficient and the spatial variability within the concrete cover. The first one, i.e., the uncertainty of the ionic diffusion coefficient, refers to the fact that a strict determination of its theoretical value is not available in reality, since the ionic diffusion in concrete might be affected by porosity, pore size distribution, and saturation degree [32,33]. As a result, some empirical values derived from a rapid migration or immersion test have to be assigned typically for the chloride ion. There is much less relevant data in the literature about the diffusion coefficients of other cations and anions including  $Na^+$ . This problem tends to be a major

cause for the numerical modeling lagging behind the experimental tests in the case of the ECE. It is worthwhile to point out that, though being challenging, the use of some advanced skills such as first-principle calculation or molecular dynamics simulation might provide new ideas for addressing this issue [34–36]. In order to demonstrate the significant influence of the ionic diffusion coefficient, a trivial computation is presented. More specifically, the original value  $D_{\text{Na}} = 0.3 \times 10^{-12} \text{ m}^2/\text{s}$  as listed in Table 1 might be replaced by  $D_{\text{Na}} = 3 \times 10^{-12} \text{ m}^2/\text{s}$ . Results in Figure 9 indicate that the discrepancies between modelling and the experimental test have been alleviated. The second one, i.e., the spatial variability of concrete refers to the fact that the initial concentration profiles of ionic species show a spatial variability in concrete other than the homogeneity [37–39]. Nevertheless, the present numerical model assumes constant identical values for both of them, i.e., the initial concentrations and diffusion coefficients of ionic species. Finally, with a great advance in time and cost savings, the numerical modelling allows a novel prediction for the rate of the chloride extraction particularly during the first 4 weeks, as shown in Figure 10.

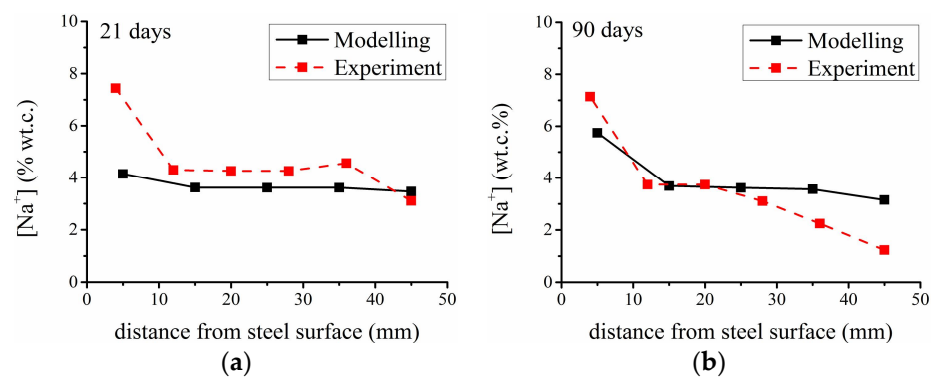


**Figure 9.** Comparison of the concentration profiles of  $\text{Na}^+$  between modelling and the experimental test with  $D_{\text{Na}} = 3 \times 10^{-12} \text{ m}^2/\text{s}$  after the electrochemical treatment of (a) 21 days; (b) 90 days.

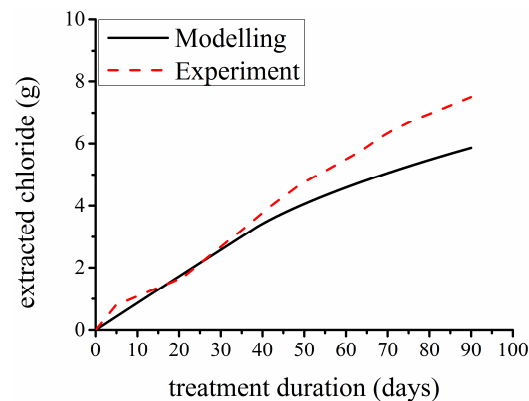


**Figure 10.** Comparison between modelling and the experimental test for the extracted amount of  $\text{Cl}^-$ .

## 5. Concluding Remarks

In this paper, a numerical study is performed about the electrochemical treatment of chloride-contaminated reinforced concrete. In particular, a classical multiple ionic transport model is introduced and solved by means of a finite difference algorithm. The effects of some critical factors are then discussed in detail. Some general remarks are given as follows.

- (1) For experimental tests of the ECE, the treatment duration might not last more than 8 weeks with an appropriate current density of  $1\text{--}3 \text{ A}/\text{m}^2$ . If only the efficiency is considered, there is no specific requirement about the cover thickness.
- (2) The overall trend of the numerical results agrees well with the experimental test for the chloride extraction, which suggests the feasibility of the current modeling scheme.

- (3) It is worthwhile to point out that several issues need to be further addressed for a more fundamental investigation. The convergence condition shall be presented. In addition, two factors shall be defined, i.e., the uncertainty of the ionic diffusion coefficient and the spatial variability within the concrete cover.

**Author Contributions:** Conceptualization, Y.G., W.L. and D.L.; methodology, Y.X. and Y.G.; investigation, Y.X.; writing—original draft preparation, Y.X.; writing—review and editing, Y.X.; revision, Y.G.; supervision, W.L. and D.L. All authors have read and agreed to the published version of the manuscript.

**Funding:** This research was funded by the National Natural Science Foundation of China (Grant Nos. U2040222, 52078123).

**Institutional Review Board Statement:** Not applicable.

**Informed Consent Statement:** Not applicable.

**Conflicts of Interest:** The authors declare no conflict of interest.

## References

1. Glass, G.K.; Buenfeld, N.R. The presentation of the chloride threshold level for corrosion of steel in concrete. *Corros. Sci.* **1997**, *39*, 1001–1013. [[CrossRef](#)]
2. Poupard, O.; Ait-Mokhtar, A.; Dumargue, P. Corrosion by chlorides in reinforced concrete: Determination of chloride concentration threshold by impedance spectroscopy. *Cem. Concr. Res.* **2004**, *34*, 991–1000. [[CrossRef](#)]
3. Ann, K.Y.; Song, H.-W. Chloride threshold level for corrosion of steel in concrete. *Corros. Sci.* **2007**, *49*, 4113–4133. [[CrossRef](#)]
4. Angst, U.M.; Elsener, B.; Larsen, C.K.; Vennesland, Ø. Chloride induced reinforcement corrosion: Electrochemical monitoring of initiation stage and chloride threshold values. *Corros. Sci.* **2011**, *53*, 1451–1464. [[CrossRef](#)]
5. Marcotte, T.; Hansson, C.; Hope, B. The effect of the electrochemical chloride extraction treatment on steel-reinforced mortar Part I: Electrochemical measurements. *Cem. Concr. Res.* **1999**, *29*, 1555–1560. [[CrossRef](#)]
6. Marcotte, T.; Hansson, C.; Hope, B. The effect of the electrochemical chloride extraction treatment on steel-reinforced mortar Part II: Microstructural characterization. *Cem. Concr. Res.* **1999**, *29*, 1561–1568. [[CrossRef](#)]
7. Otero, E.; González, J.A.; Cobo, A.; González, M.D.L.N. Electrochemical chloride removal from reinforced concrete structures and its ability to repassivate prerusted steel surfaces. *Mater. Corros.* **2001**, *52*, 581–589. [[CrossRef](#)]
8. Siegwart, M.; Lyness, J.F.; McFarland, B.J. Change of pore size in concrete due to electrochemical chloride extraction and possible implications for the migration of ions. *Cem. Concr. Res.* **2003**, *33*, 1211–1221. [[CrossRef](#)]
9. Orellan Herrera, J.C.; Escadeillas, G.; Arliguie, G. Electro-chemical chloride extraction: Influence of C3A of the cement on treatment efficiency. *Cem. Concr. Res.* **2006**, *36*, 1939–1946. [[CrossRef](#)]
10. Garcés, P.; De Rojas, M.S.; Climent, M. Effect of the reinforcement bar arrangement on the efficiency of electrochemical chloride removal technique applied to reinforced concrete structures. *Corros. Sci.* **2006**, *48*, 531–545. [[CrossRef](#)]
11. Yeih, W.; Chang, J.J.; Hung, C.C. Selecting an adequate procedure for the electrochemical chloride removal. *Cem. Concr. Res.* **2006**, *36*, 562–570. [[CrossRef](#)]
12. Miranda, J.; Cobo, A.; Otero, E.; González, J. Limitations and advantages of electrochemical chloride removal in corroded reinforced concrete structures. *Cem. Concr. Res.* **2007**, *37*, 596–603. [[CrossRef](#)]
13. Orellan, J.; Escadeillas, G.; Arliguie, G. Electrochemical chloride extraction: Efficiency and side effects. *Cem. Concr. Res.* **2004**, *34*, 227–234. [[CrossRef](#)]
14. Nguyen, T.H.Y.; Tran, V.M.; Pansuk, W.; Cao, N.T.; Bui, V.H.L. Electrochemical chloride extraction on reinforced concrete contaminated external chloride: Efficiencies of intermittent applications and impacts on hydration products. *Cem. Concr. Compos.* **2021**, *121*, 104076. [[CrossRef](#)]
15. Abdelaziz, G.; Abdelalim, A.; Fawzy, Y. Evaluation of the short and long-term efficiencies of electro-chemical chloride extraction. *Cem. Concr. Res.* **2009**, *39*, 727–732. [[CrossRef](#)]
16. Pérez, A.; Climent, M.A.; Garcés, P. Electrochemical extraction of chlorides from reinforced concrete using a conductive cement paste as the anode. *Corros. Sci.* **2010**, *52*, 1576–1581. [[CrossRef](#)]
17. Cañón, A.; Garcés, P.; Climent, M.A.; Carmona, J.; Zornoza, E. Feasibility of electrochemical chloride extraction from structural reinforced concrete using a sprayed conductive graphite powder–cement paste as anode. *Corros. Sci.* **2013**, *77*, 128–134. [[CrossRef](#)]
18. Carmona, J.; Garcés, P.; Climent, M.A. Efficiency of a conductive cement-based anodic system for the application of cathodic protection, cathodic prevention and electrochemical chloride extraction to control corrosion in reinforced concrete structures. *Corros. Sci.* **2015**, *96*, 102–111. [[CrossRef](#)]
19. Andrade, C.; Dies, J.M.; Alamán, A.; Alonso, C. Mathematical modelling of electrochemical chloride extraction from concrete. *Cem. Concr. Res.* **1995**, *25*, 727–740. [[CrossRef](#)]

20. Castellote, M.; Andrade, C.; Alonso, C. Electrochemical chloride extraction: Influence of testing conditions and mathematical modelling. *Adv. Cem. Res.* **1999**, *11*, 63–80. [[CrossRef](#)]
21. Castellote, M.; Andrade, C.; Alonso, C. Electrochemical removal of chlorides: Modelling of the extraction, resulting profiles and determination of the efficient time of treatment. *Cem. Concr. Res.* **2000**, *30*, 615–621. [[CrossRef](#)]
22. Buenfeld, N.R.; Glass, G.K.; Hassanein, A.M.; Zhang, J.-Z. Chloride Transport in Concrete Subjected to Electric Field. *J. Mater. Civ. Eng.* **1998**, *10*, 220–228. [[CrossRef](#)]
23. Li, L.Y.; Page, C.L. Modelling of electrochemical chloride extraction from concrete: Influence of ionic activity coefficients. *Comput. Mater. Sci.* **1998**, *9*, 303–308. [[CrossRef](#)]
24. Li, L.; Page, C. Finite element modelling of chloride removal from concrete by an electrochemical method. *Corros. Sci.* **2000**, *42*, 2145–2165. [[CrossRef](#)]
25. Liu, Q.-F.; Li, L.-Y.; Easterbrook, D.; Yang, J. Multi-phase modelling of ionic transport in concrete when subjected to an externally applied electric field. *Eng. Struct.* **2012**, *42*, 201–213. [[CrossRef](#)]
26. Liu, Q.-F.; Easterbrook, D.; Yang, J.; Li, L.-Y. A three-phase, multi-component ionic transport model for simulation of chloride penetration in concrete. *Eng. Struct.* **2015**, *86*, 122–133. [[CrossRef](#)]
27. Liu, Q.-F.; Feng, G.-L.; Xia, J.; Yang, J.; Li, L.-Y. Ionic transport features in concrete composites containing various shaped aggregates: A numerical study. *Compos. Struct.* **2018**, *183*, 371–380. [[CrossRef](#)]
28. Sergi, G.; Yu, S.W.; Page, C.L. Diffusion of chloride and hydroxyl ions in cementitious materials exposed to a saline environment. *Mag. Concr. Res.* **1992**, *44*, 63–69. [[CrossRef](#)]
29. Fajardo, G.; Escadeillas, G.; Arliguie, G. Electrochemical chloride extraction (ECE) from steel-reinforced concrete specimens contaminated by “artificial” sea-water. *Corros. Sci.* **2006**, *48*, 110–125. [[CrossRef](#)]
30. Toumi, A.; François, R.; Alvarado, O. Experimental and numerical study of electrochemical chloride removal from brick and concrete specimens. *Cem. Concr. Res.* **2007**, *37*, 54–62. [[CrossRef](#)]
31. Yang, J.B.; Wittmann, F.H.; Zhao, T.J.; Yan, P.Y. Experimental research of chloride diffusion coefficient in concrete. *J. Build. Mater.* **2007**, *10*, 223–228. (In Chinese)
32. Chatterji, S. Evidence of variable diffusivity of ions in saturated cementitious materials. *Cem. Concr. Res.* **1999**, *29*, 595–598. [[CrossRef](#)]
33. Sun, Y.-M.; Liang, M.-T.; Chang, T.-P. Time/depth dependent diffusion and chemical reaction model of chloride transportation in concrete. *Appl. Math. Model.* **2012**, *36*, 1114–1122. [[CrossRef](#)]
34. Zhou, Y.; Hou, D.; Jiang, J.; Wang, P. Chloride ions transport and adsorption in the nano-pores of silicate calcium hydrate: Experimental and molecular dynamics studies. *Constr. Build. Mater.* **2016**, *126*, 991–1001. [[CrossRef](#)]
35. Jiang, J.; Wang, P.; Hou, D. The mechanism of cesium ions immobilization in the nanometer channel of calcium silicate hydrate: A molecular dynamics study. *Phys. Chem. Chem. Phys.* **2017**, *19*, 27974–27986. [[CrossRef](#)] [[PubMed](#)]
36. Wang, P.; Zhang, Q.; Wang, M.; Yin, B.; Hou, D.; Zhang, Y. Atomistic insights into cesium chloride solution transport through the ultra-confined calcium–silicate–hydrate channel. *Phys. Chem. Chem. Phys.* **2019**, *21*, 11892–11902. [[CrossRef](#)]
37. Angst, U.M.; Polder, R. Spatial variability of chloride in concrete within homogeneously exposed areas. *Cem. Concr. Res.* **2014**, *56*, 40–51. [[CrossRef](#)]
38. Castaldo, P.; Gino, D.; Carbone, V.I.; Mancini, G. Framework for definition of design formulations from empirical and semi-empirical resistance models. *Struct. Concr.* **2018**, *19*, 980–987. [[CrossRef](#)]
39. Castaldo, P.; Gino, D.; Marano, G.C.; Mancini, G. Aleatory uncertainties with global resistance safety factors for non-linear analyses of slender reinforced concrete columns. *Eng. Struct.* **2022**, *255*, 113920. [[CrossRef](#)]